Reaction Pathways of Photoexcited Retinal in Proteorhodopsin Studied by Pump−Dump−Probe Spectroscopy

Alisa Rupenyan,[†] Ivo H. M. van Stokkum,[†] Jos C. Arents,[‡] Rienk van Grondelle,[†] Klaas J. Hellingwerf,[†,‡] and Marie Louise Groot*[,†]

Department of Physics and Astronomy, Faculty of Sciences, Vrije Universiteit, De Boelelaan 1081, 1081 HV Amsterdam, The Netherlands, and Laboratory for Microbiology, Swammerdam Institute for Life Sciences, University of Amsterdam, Nieuwe Achtergracht 166, 1010 WV Amsterdam, The Netherlands

Received: July 10, 2009; Revised Manuscript Received: October 26, 2009

Proteorhodopsin (pR) is a membrane-embedded proton pump from the microbial rhodopsin family. Light absorption by its retinal chromophore initiates a photocycle, driven by *trans*/*cis* isomerization on the femtosecond to picosecond time scales. Here, we report a study on the photoisomerization dynamics of the retinal chromophore of pR, using dispersed ultrafast pump−dump−probe spectroscopy. The application of a pump pulse initiates the photocycle, and with an appropriately tuned dump pulse applied at a time delay after the dump, the molecules in the initial stages of the photochemical process can be de-excited and driven back to the ground state. In this way, we were able to resolve an intermediate on the electronic ground state that represents chromophores that are unsuccessful in isomerization. In particular, the fractions of molecules that undergo slow isomerization (20 ps) have a high probability to enter this state rather than the isomerized K-state. On the ground state reaction surface, return to the stable ground state conformation via a structural or vibrational relaxation occurs in 2−3 ps. Inclusion of this intermediate in the kinetic scheme led to more consistent spectra of the retinal-excited state, and to a more accurate estimation of the quantum yield of isomerization ($\Phi = 0.4$ at pH 6).

Introduction

Proteorhodopsins (pR's) are members of the large family of microbial rhodopsins.[1] They are widely distributed in marine proteobacteria and spectrally tuned to the light climate in their oceanic environment, which has led to the evolution of blue- and green-light absorbing variants. Their contribution to the conservation of solar energy in the biosphere is significant.[2] Furthermore, pR and charged lipids spontaneously assemble *in vitro* into long-range-ordered 2D arrays which hold promises for technological applications.[3]

Green-light absorbing proteorhodopsin, the subject of this investigation, functions as a light-driven proton pump by creating a proton gradient from the extracellular to the cytoplasmic side of the membrane. Similar to bacteriorhodopsin, the absorption of light by the chromophore of pR, a retinal molecule covalently linked to the apoprotein through a protonated Schiff base, initiates *E*/*Z* (or all-*trans* to 13-*cis*) chromophore isomerization. This leads to a series of thermal transitions during which the proton from the Schiff base is transferred to the counterion formed by Asp97, Asp227, and a bound water molecule.[4−6] The Schiff base is subsequently reprotonated by a proton from Glu108, localized on the cytoplasmic surface. Proteorhodopsin lacks the ionizable residues corresponding to Glu194 and Glu204 of bacteriorhodopsin, thought to be involved in the proton release pathway at the extracellular surface, which leaves the exit route of pumped protons in pR uncertain.

The light-induced isomerization in pR has previously been studied by femtosecond fluorescence and pump−probe spectroscopy in the visible and in the mid-IR.[7−9] The quantum yield of the reaction is ∼0.65 at pH 9.5 and ∼0.5 at pH 6.5,[9] which implies that the initially excited population can either evolve to the isomerized product or relax back to the original *trans* ground state configuration. Most of the product is formed on the faster time scales (∼0.2−2 ps), whereas a small fraction is formed on an ∼20 ps time scale. Already at the ultrafast time scales the retinal isomerization also affects the surrounding protein backbone, that possibly undergoes a conformational change, as revealed by a change in amide band absorption.[7,9]

The mutation of a single residue close to the retinal chromophore, Gln105, can shift the absorption of blue pR, to mimic green pR.[10] The role of the protein environment is also important in the photochemistry of the chromophore. Small structural differences between different rhodopsins have a significant effect on the rate and mechanism of retinal isomerization. Furthemore, the isomerization of retinal in solution is slower and nonselective, i.e., can take place around different double bonds, with the photoproduct being formed in 1−2 ps[11] and a quantum yield 2−3 times less than in bacteriorhodopsin.[12,13] In the chromophore-binding pocket of visual rhodopsin, photoisomerization is completed in ∼0.2 ps,[14] and in bacteriorhodopsin in 0.55 ps.[15] In pR, the formation of the 13-*cis* state (K-state) occurs multiexponentially, on time scales spanning from hundreds of femtoseconds to tens of picoseconds. Proteorhodopsin at slightly alkaline pH, close to pR's natural environment, has a slightly higher quantum yield and faster rate constants. At pH 6, where the Schiff base counterion Asp97 is protonated, the reaction is less efficient, probably due to the altered charge distribution in the retinal pocket.[8,9,16] However, the reaction mechanism is not altered by the pH of the

* To whom correspondence should be addressed. Phone: +31-(0)20-598 2570. Fax: +31-(0)20-598 7999. E-mail: ML.Groot@few.vu.nl.
[†] Vrije Universiteit.
[‡] University of Amsterdam.

10.1021/jp9065289
Published on Web 11/23/2009

environment, and the transient absorption data of pR in alkaline and acidic environment can be interpreted using the same model for the dynamics of the isomerization.[9]

Although the excited state evolution of retinal in proteorhodopsin has been characterized, more information on what determines the quantum yield of its photoisomerization can be obtained from monitoring the relative progress on the excited state potential and looking at the dynamics on the ground state potential energy surface, using pump−dump−probe spectroscopy. The pump−dump−probe experimental technique consists of the administration of an additional (dump) pulse to the sample, in the spectral region of the stimulated emission, delayed with respect to the excitation (i.e., pump) pulse.[17−21] This pulse causes depletion of the excited state population, sending part of it back to the ground state. During the delay time between the pump and the dump pulses, the excited state population evolves on the reaction surface, and after dumping the population evolves on the ground state potential energy surface. In this way, the dynamics and reaction pathways on the ground state and the excited state can be monitored. Pump−dump−probe spectroscopy, probing at a single wavelength in the region of the stimulated emission has been applied to bacteriorhodopsin, resolving induced absorption in the near-IR, attributed to the excited state previously hidden by overlap with the stimulated emission.[22] In another study on bacteriorhodopsin, it was found that the dumped population does not continue on in the photocycle.[17]

Application of dispersed pump−dump−probe (or stimulated emission depletion) spectroscopy to photoactive yellow protein (PYP), a bacterial photoreceptor from *Halorhodospira halophila*,[23] revealed a ground state intermediate (GSI) in PYP, the detection of which until then was hindered by overlap with stimulated emission.[24] This intermediate results from those molecules in which the chromophore is not able to productively isomerize, because of the inability to disrupt a hydrogen bond between the chromophore and the protein.[25] Thus, molecules that are not able to enter the photocycle can return from the excited state to the ground state either directly or indirectly via this ground state intermediate (GSI) on the relaxation pathway.

Here, we report a pump−dump−probe study of proteorhodopsin in a slightly acidic (pH 6), detergent-containing buffer. By applying dispersed pump−dump−probe spectroscopy, we are able to monitor the dump-induced changes at wavelengths from 450 to 750 nm. Simultaneous global analysis of pump−probe data and pump−dump−probe data, collected at different dump delays, enables us to develop a more complete reaction model for photoactivation of proteorhodopsin that includes the ground state dynamics, and reveals the reaction pathway of those retinal chromophores that are not able to accomplish productive isomerization.

Materials and Methods

Proteorhodopsin was isolated from *E. coli* UT5600/pBetacaro/pKJ829-proteo, a strain kindly provided by Dr. K. H. Jung (Department of Life Science, Sogang University, Seoul, Korea). Membranes containing holo-pR were isolated by resuspending harvested *E. coli* cells in about 1% culture volume of 20 mM Tris buffer pH 7.5, containing 500 mM NaCl, 0.1% (w/v) dodecyl-maltoside (DM), and 20 mM imidazole. After thawing and addition of 1 mg/mL lysozyme, 25 μg/mL DNase I, 25 μg/mL RNase, and a protease inhibitor cocktail, cells were disrupted by sonication. Cell debris was removed by low speed centrifugation (10 min at 3000*g*) and the cytoplasmic membranes in the supernatant were solubilized in detergent (1.5% (w/v) DM) overnight via slow stirring at 4 °C. After 10 min of centrifugation at 10000*g*, pR was purified using a HisTrap FF crude column (GE Healthcare, Eindhoven, The Netherlands), in combination with an imidazole gradient. Finally, the purified pR was dialyzed against 0.5 M NaCl, 0.1% (w/v) DM, plus 25 mM MES buffer at pH 6.[9]

Samples consisted of a protein solution contained in a 2 mm quartz cuvette. The OD of the sample was 0.3 at the maximum of the absorption spectrum (530 nm). This absorption maximum is consistent with values reported in the literature for pR at pH 6.[26]

The experimental setup consisted of an integrated Ti:sapphire oscillator-regenerative amplifier laser system (Coherent Legend-UHP) operating at 1 kHz and at a central wavelength of 800 nm, producing 85 fs pulses of 2.5 mJ. Part of this 800 nm light was introduced into a commercial OPERA (Coherent) system to generate the 510 nm excitation pulse. The second portion of the 800 nm light was focused into a laterally rotating CaF_2 plate to generate white light for the probe. The probe pulses were spatially overlapped with the excitation beam in the sample using reflective optics. After overlap in the sample, the probe was dispersed by a 15 cm focal length spectrograph (Oriel) onto a home-built photodiode array detector. The polarization of the excitation pulse was set to the magic angle (54.7°) with respect to the probe pulses. A phase-locked chopper, operating at 500 Hz, ensured that at every other shot the sample was excited and an absorbance difference spectrum could be calculated. To ensure a fresh spot for each laser shot, the quartz cuvette was repositioned by shaking. The power of the excitation pulses was 200 nJ. The instrument response function was ∼130 fs.

For the three-pulse pump−dump−probe measurements, part of the pump line was branched off before the OPERA, and the 800 nm pulses were introduced into a second commercial OPERA system (Coherent) to produce a 700 nm dump pulse of 200 nJ. A second delay line in the path of the dump pulse allowed for the timing of the dump pulse with respect to the pump pulse. A second chopper, placed in the path of the dump pulse, was used to ensure the acquisition of dumped and nondumped spectra. This chopper, together with the pump chopper, was set to rotate asynchronously, resulting in a quasi-simultaneous measurement of a set of four discrete signals: (A) pump on and dump on (referred to as pump−dump−probe data set, PDP); (B) pump on and dump off (referred to as pump−probe data set, PP); (C) pump off and dump on; (D) pump off and dump off. This way of collecting data ensured that all measurements were carried out under the same conditions. We performed measurements at dump delays of 0.5, 2, 5, and 10 ps, respectively.

The data were subjected to global analysis.[27] Cross-phase modulation (xpm) was modeled by a component with the time profile of the instrument response function (IRF).

Results

An overlay of the steady state spectrum of pR with the pump pulse (510 nm), the dump pulse (700 nm), and the transient absorption of a sample, taken at 0.55 ps after excitation, is shown in Figure 1. The dump pulse was chosen to overlap with the stimulated emission band but not with the steady state absorption of the protein. Upon dumping, two possible outcomes are anticipated: if there is no higher excited state absorption that coincides with the dump wavelength, a fraction of the molecules in their excited state will be de-excited, i.e., sent back to the ground state. Alternatively, molecules in their excited state can absorb another photon, to be sent to a higher excited state.

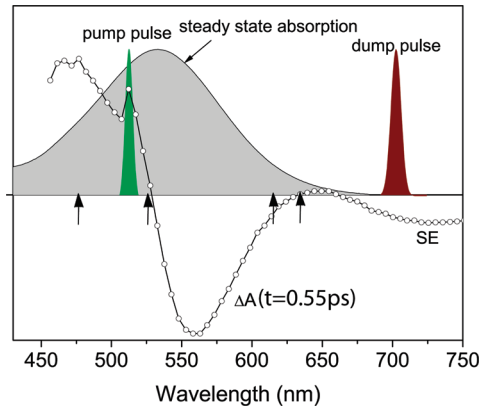

Figure 1. Steady state absorption spectrum of pR, overlaid with the transients at $t = 0.55$ ps and the spectra of the pump and the dump pulses. All spectra have been normalized. The arrows indicate wavelengths of the time traces presented in Figure 2.

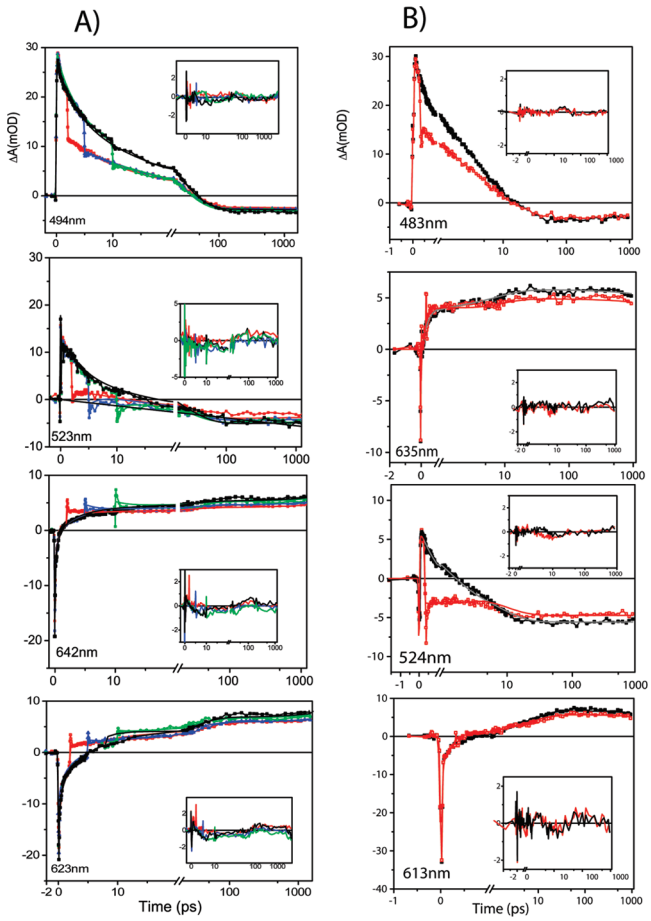

Figure 2. (A) Pump−dump−probe time traces at dump delays of 2, 5, and 10 ps, together with pump−probe time traces at selected wavelengths (i.e., 494, 523, 642, and 623 nm) for pR at pH 6. (B) Pump−dump−probe time traces at a dump delay of 0.5 ps, together with pump−probe time traces at 484, 524, 635, and 613 nm. The insets represent residuals, color-coded to the corresponding data sets. The fits and the residuals are derived from the application of the target model, shown in Figure 4.

Therefore, the wavelength of the dump pulse is very important for the outcome of the dumping. Significantly, none of the ultrafast studies of pR report excited state absorption in the spectral region around 700 nm[8,9,16] (see also Figure 1).

We applied dump pulses at delay times of 0.5, 2, 5, and 10 ps between the pump and the dump pulse. Representative time traces are shown in Figure 2, together with reference time traces recorded without the application of the dump pulse. Following the application of the dump pulse, a clear instantaneous depletion of the excited state absorption signals is observed in the traces at 494 and 523 nm, as well as the appearance of induced absorption signals, which are red-shifted compared to the ground state absorption (see the time trace at 623 nm). These signals disappear in ∼5 ps, and the dump pulse leads to lower final-product absorption, as can be seen from the lower signals at long delay times (Figure 2). This effect is most clearly observed in the data set with a dump pulse applied 0.5 ps after the pump pulse (which have therefore been represented separately), and almost absent in the data set with a dump pulse applied at 10 ps. This observation indicates that the pR excited state is heterogeneous, in agreement with earlier findings[9,28] and that from the longer-lived excited states less K-state is produced.

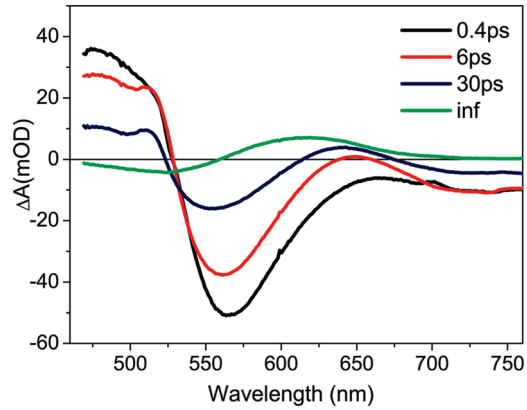

Figure 3. Evolution-associated difference spectra, derived from a sequential analysis of the data. The decay times of the EADS are shown in the inset to the figure.

Sequential Analysis of Pump−Probe Data. First, we analyzed the pump−probe time traces of all data sets using a simple sequential scheme, with increasing exponential lifetimes, which yielded time constants of 0.4, 6, and 30 ps and a nondecaying component. In our previous study, similar time constants were sufficient to describe the transient absorption changes with a sequential model.[9] The corresponding evolution-associated difference spectra (EADS) are shown in Figure 3. The initial EADS (black), with a lifetime of 0.4 ps, is characterized by induced absorption, blue-shifted from the ground state bleach, peaking at ∼470 nm, a ground state bleach, which is maximal at 560 nm, and a broad stimulated emission band at wavelengths >600 nm. The signal in the stimulated emission region is reduced after the first 0.4 ps, and located in the region from 650 to 760 nm. Both the excited state absorption and the stimulated emission decay multiexponentially with time constants of 0.4, 6, and 30 ps, accompanied by the rise of the positive signal at ∼645 nm (red and blue EADS). In the final (green) spectrum, the positive signal has developed into a band peaking at ∼620 nm. This final spectrum can be attributed to the sum of the bleached ground state absorption, plus absorption due to product formation. This spectrum corresponds to the absorption-difference spectrum of the K-intermediate in the photocycle of pR,[6] which has an isomerized, 13-*cis* retinal chromophore. The decay times of the excited state of pR at pH 6 are in reasonable agreement with the decay times of 0.2, 2, and 18 ps observed in our earlier pump−probe study,[9] and with previously reported time constants associated with the pR multiexponential excited state decay, derived from pump−probe experiments in the visible (1 and 16 ps at pH 6[16,28]) and in the mid-IR (0.5, 2, and 11 ps at pH 9.5[7]).

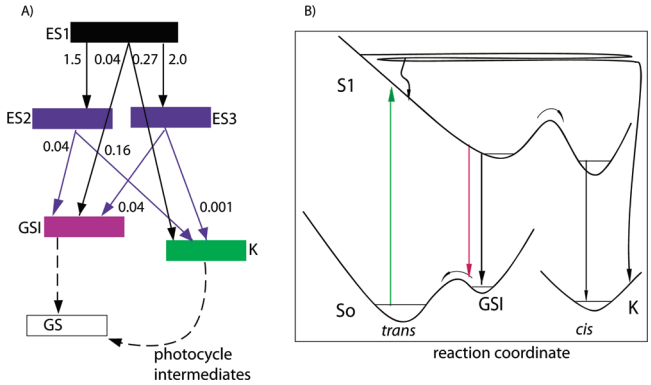

Figure 4. (A) Schematic representation of the target model used for the analysis of the data. The arrows represent transitions with associated rate constants in ps^{-1}, and the squares represent states, color-coded to the SADS shown in Figure 5. (B) Sketch of the potential energy surfaces, corresponding to the target model that was applied for analysis of the data. The green arrow indicates the excitation of molecules from the ground state by the pump pulse; the red arrow indicates the de-excitation of molecules in the excited state due to the dump pulse. The GSI and K-state reside on different reaction coordinates.

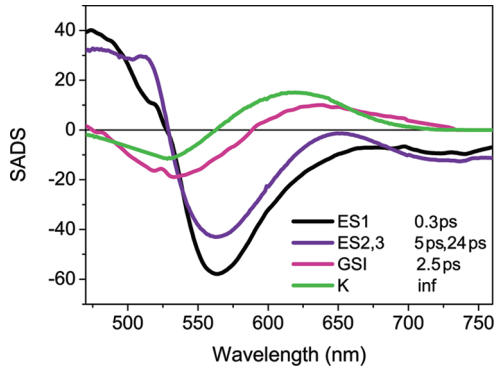

Figure 5. Species-associated difference spectra (SADS), estimated from the simultaneous application of the target model shown in Figure 4A to pump−probe and pump−dump−probe data, at multiple delay times of the dump pulse. The inset in the figure shows the lifetimes of the species. The SADS are color-coded according to the model depicted in Figure 4A.

Target Analysis of Pump−Probe and Pump−Dump−Probe Data. The spectra obtained by analysis with a sequential scheme reflect the mixtures of intermediates that exist simultaneously for periods of time, defined by the formation and decay rate of each intermediate, rather than spectra associated with physically distinct species. We therefore applied a physically relevant model to the data to obtain pure species-associated difference spectra (SADS). In this analysis, all of the pump−dump−probe and pump probe data sets were analyzed simultaneously, which led to significant improvement of the signal-to-noise ratio of the results. The model, shown in Figure 4, is partially based on the model that we employed previously.[9] It comprises three excited state species (ES1, ES2, ES3) to account for the multiphasic decay of the excited state, a transient ground state (GSI), and a species corresponding to the product state (K). Each of the three excited states can form product K, or decay to the ground state via the transient ground state intermediate, GSI. To simplify the model, and because in a first try the spectra of ES2 and ES3 were virtually identical, the spectra of the ES2 and ES3 are equated (violet SADS in Figure 5). They are characterized by a red shift of part of the stimulated emission in the 600−700 nm region, as compared to the SADS of ES1. This heterogeneous model provides a direct way to assess the amount of product formed with each time constant and from each ES component. Physically, it may represent heterogeneity in the structure of the retinal-binding pocket that affects the ability of the chromophore to isomerize. The species-associated difference spectrum of each component is shown in Figure 5.

TABLE 1: Contributions of Each Excited State to the Product Yield (Yield of the K-State) and the Yield of the Ground State Intermediate (GSI Yield), Estimated from Target Analysis of the Data with the Model Shown in Figure 4

	population	ES2	ES3	K	GSI
ES1	1	0.39	0.52	0.08	0.01
ES2	0.39			0.30	0.08
ES3	0.52			0.02	0.51
K-yield				0.40	
GSI yield					0.60

The instantaneous depletion of the ES absorption at time delays of 0.5, 2, 5, and 10 ps after time zero, induced by the dump pulse, is modeled as an instantaneous loss of population (50−70%) from the excited states ES2 and ES3 and a gain of population of a newly formed intermediate, referred to as a ground state intermediate (GSI). The spectrum of this species is characterized by a ground state bleach and positive absorption band at wavelengths longer than ∼600 nm (magenta SADS in Figure 5). The GSI has a lifetime of 2.5 ps, and its absorption is red-shifted with respect to the ground state, partially overlapping with the stimulated emission. If the GSI is not taken into account in the analysis of pump−probe data, it manifests itself as a positive feature centered at 600 nm in the SADS of the excited states.[9] In contrast, if one does take it into account, this improves significantly the spectral shape of these SADS in the region of the stimulated emission.

ES1, ES2, and ES3 have the typical characteristics of pure excited state spectra (ground state bleach, blue-shifted positive absorption, and stimulated emission), without a contribution from the absorption of the product state; see Figure 5. The branching parameters of all transitions depicted in Figure 4 are shown in Table 1. Note that the product state is formed mainly on a subpicosecond to picosecond time scale, i.e., from ES1 and ES2, and that only 2% of the product is derived from the long-lived ES3. We estimated previously the quantum yield of K-state formation to be ∼0.5, based on a target analysis, plus deconvolution of the product state difference spectrum.[9] However, now that the pump−dump−probe measurements have revealed the involvement of the GSI in the deactivation pathway, a more reliable estimate of the quantum yield by target analysis can be given: 0.4.

We also tested a model allowing for additional direct transitions to the ground state on the relaxation pathway, and found that it improves neither the SADS nor the quality of the fits. The data clearly show a reduction in the K-yield upon dumping. This effect is especially notable when the dump pulse is applied early, since it is the short-lived excited states that produce virtually all K. The reduction in K-yield indicates that from the GSI no product is being formed, or at least not to a significant extent. Our current model assumes no K-formation from the GSI, and with that, a spectrum for the GSI is returned that looks very reasonable in relative size of its bleach and product band absorption to that of the K-state (note that from the target analysis "true" spectra result, not affected by issues as relative yields). We further attempted to analyze our mid-IR data[9] with this model. However, due to the simultaneous coexistence of the ground state intermediate and the excited and product states, the spectral shape of the GSI could not be

unambiguously assigned. Therefore, future pump−dump−probe experiments, probing in the mid-IR, are necessary to obtain the mid-IR spectrum of the GSI.

Discussion

The simultaneous acquisition of pump−probe and pump−dump−probe data has allowed for a more detailed model for the reaction dynamics of photoisomerization of retinal in pR. A previously undetected intermediate state on the ground state potential has now been resolved and more reliable ES spectra have been obtained, which has led to the improved estimate of the isomerization quantum yield of 0.4.

In pR, the excited state decay and the formation of the *cis*-product state are multiphasic processes.[8,9,16] Since we do not observe spectral evolution in the excited state absorption after the initial subpicosecond phase, we assign the multiexponentiality of the excited state decay to structural heterogeneity of the retinal and the surrounding protein. Heterogeneity in bacteriorhodopsin has been suggested previously to result from conformational plasticity of the protein that would modify the structure around the chromophore and result in a distribution of rate constants for the decay of the excited state.[29] Recently, the simultaneous existence of several 13-*cis*, 15-*syn* states (representing slightly different conformations in the neighborhood of the Schiff-base linkage) in dark-adapted bacteriorhodopsin has been directly observed by solid state NMR experiments,[30] as well as heterogeneity within several of the cryotrapped intermediates.[31] Here, we show that heterogeneity leads to "primed" chromophores that isomerize fast and "not-primed" chromophores that isomerize slowly and with low yield. Similar observations have been made for the chromophore dynamics in PYP.[24]

Our measurements can be described by a model for the excited state dynamics that is similar to that for other retinal molecules, except for the fact that the heterogeneity in pR is larger: Upon absorption of a photon, the wave packet that is created initially oscillates on the high vibrational levels of S_1, and, within 0.3−0.4 ps, relaxes via intramolecular vibrational energy redistribution, due to structural evolution of the excited state population along multiple low-frequency modes that carry the molecule out of the harmonic photochemically inactive Franck−Condon region, into the photochemically active geometry. A similar sequence of reactions has been observed in bacteriorhodopsin using stimulated Raman spectroscopy,[31] and is responsible for the observed shift of the stimulated emission. Red-shifted and broad bands, corresponding to vibrationally hot states, are also observed in the mid-IR spectra of the excited states of pR.[7,9] During the lifetime of the initial vibrationally hot excited state, the chromophore may evolve along its reaction coordinates to form either a *cis*-isomerized product (Figure 4) or the ground state intermediate, and return to the ground state conformation.

The same scenario holds for the two excited states formed after relaxation of the initial excited state: they can either undergo transition to the *cis* state or return to the initial ground state conformation via the ground state intermediate. The long lifetime of ES3 (24 ps) cannot be explained by vibrational cooling, and points to the crossing of a significant potential-energy barrier on the excited state potential surface that slows down the reaction, indicating that ES3 is structurally different from ES1 and ES2, as indicated by the vibrational spectra of the excited states of pR.[9] As much as 50% of the excited states have this exceptionally long lifetime, and these states have a K-yield of only 2% (see Table 1). The rate to the K-state of ES3 we find is only 0.001 ps^{-1}, as compared to 0.16 ps^{-1} for ES2 (and 0.27 ps^{-1} for ES1). The barrier for K-formation from ES3 is therefore significantly higher than for ES2, and the difference can be estimated, using these rates and the Boltzman expression, to ∼125 meV. This may point to structural rearrangements that hinder the isomerization, as our previous mid-IR studies of pR isomerization showed that the proteins in the long-living excited state were characterized by a spectral change in the amide II region.[7,9]

The SADS of the GSI that we resolve upon the simultaneous analysis of pump−probe and pump−dump−probe data has the shape of the sum of the ground state bleach plus a positive absorption band, red-shifted with respect to the ground state absorption but blue-shifted with respect to the stimulated emission (magenta SADS in Figure 5). The population of this state is significantly enhanced in the pump−dump−probe data but hidden by overlap with the stimulated emission and the product state absorption in the pump−probe data. We note that the combined analysis of the pump−probe and pump−dump−probe data results in a kinetic model that includes the GSI as a normal intermediate in the relaxation pathway; i.e., the GSI is present on the normal relaxation pathway of the retinal molecules, also without forced de-excitation due to the dump pulse. Population of the GSI leads only to the reformation of the GS, and not to K-state formation. This is similar to the observations made in bacteriorhodopsin and PYP, i.e., that the dumped state is biologically inactive.[17,24]

The blue shift of the GSI absorption with respect to the stimulated emission may indicate that upon dumping a very fast relaxation occurs on the ground state, that we have not time-resolved in the current experiment. The red-shifted absorption of the GSI with respect to the ground state absorption, notably even further red-shifted than the K-state absorption, would correspond to an intermediate with a lower frequency of the C═C stretch vibration in the mid-IR, according to a reported correlation of the vibrational frequencies of retinal with visible absorption maxima.[32] This might indicate that the GSI is also in a *cis*-conformation, similar to the product state K.[7,9] Considering a GSI lifetime of only 2.5 ps, and its absorption properties, it can be related to molecules that undergo unsuccessful attempts to fully isomerize and decay to the ground state from a distorted or twisted *cis*-conformation that needs to relax in order to assume the ground state conformation. Moreover, a distorted cryo-trapped K-like state of bacteriorhodopsin has recently also been observed[30] by solid state NMR spectroscopy. On the other hand, via dumping, a nonequilibrium ground state population, i.e., a vibrationally "hot" all-*trans* ground state, may be formed. In both cases, the 2.5 ps dynamic process represents evolution on the ground state potential energy surface, represented in Figure 4 as a potential barrier on the S_0 surface. It will be revealing to measure the characteristics of the structure of the GSI state with mid-infrared transient spectroscopy in future experiments.

The reason for involvement of the ground state intermediate in the return to the ground state might also originate in the protein surroundings of the chromophore. A conformational change of the protein on a picosecond time scale present in all excited states was observed in ultrafast pump−probe studies.[7,9] This conformational change is due to a response of the protein backbone, following the excitation of the retinal molecule, due to the isomerization,[9] which in turn might be related to storage of photon energy for proton transport.[7] As this amide spectral change is persistent on a time scale longer than the time of relaxation of the excited state molecules, it creates an environ-

ment for the chromophore, different from the initial ground state environment, possibly imposing steric or electrostatic constraints on the chromophore, which could translate into a barrier on the relaxation pathway.

We can now summarize the dynamics of the light-induced isomerization of retinal in pR. The initially excited molecules can follow either a productive pathway, and form a *cis*-isomer, or a relaxation pathway, returning toward the initial all-*trans* ground state via a ground state intermediate. Most of the *cis*-isomers are formed on a subpicosecond to picosecond time scale, from short-lived excited states. Conformational heterogeneity accounts for the presence of a fraction of pR proteins having chromophores with very long-lived excited states and a dramatically reduced product formation that evolve mainly on the relaxation pathway.

References and Notes

(1) Beja, O.; Aravind, L.; Koonin, E. V.; Suzuki, M. T.; Hadd, A.; Nguyen, L. P.; Jovanovich, S.; Gates, C. M.; Feldman, R. A.; Spudich, J. L.; Spudich, E. N.; DeLong, E. F. Bacterial rhodopsin: Evidence for a new type of phototrophy in the sea. *Science* **2000**, *289* (5486), 1902–1906.

(2) Beja, O.; Spudich, E. N.; Spudich, J. L.; Leclerc, M.; DeLong, E. F. Proteorhodopsin phototrophy in the ocean. *Nature* **2001**, *411* (6839), 786–789.

(3) Liang, H.; Whited, G.; Nguyen, C.; Stucky, G. D. The directed cooperative assembly of proteorhodopsin into 2D and 3D polarized arrays. *Proc. Natl. Acad. Sci. U.S.A.* **2007**, *104* (20), 8212–8217.

(4) Dioumaev, A. K.; Brown, L. S.; Shih, J.; Spudich, E. N.; Spudich, J. L.; Lanyi, J. K. Proton transfers in the photochemical reaction cycle of proteorhodopsin. *Biochemistry* **2002**, *41* (17), 5348–5358.

(5) Ikeda, D.; Furutani, Y.; Kandori, H. FTIR study of the retinal Schiff base and internal water molecules of proteorhodopsin. *Biochemistry* **2007**, *46* (18), 5365–5373.

(6) Varo, G.; Brown, L. S.; Lakatos, M.; Lanyi, J. K. Characterization of the photochemical reaction cycle of proteorhodopsin. *Biophys. J.* **2003**, *84* (2), 1202–1207.

(7) Amsden, J. J.; Kralj, J. M.; Chieffo, L. R.; Wang, X.; Erramilli, S.; Spudich, E. N.; Spudich, J. L.; Ziegler, L. D.; Rothschild, K. J. Subpicosecond Protein Backbone Changes Detected during the Green-Absorbing Proteorhodopsin Primary Photoreaction. *J. Phys. Chem. B* **2007**, *111* (40), 11824–11831.

(8) Lenz, M. O.; Huber, R.; Schmidt, B.; Gilch, P.; Kalmbach, R.; Engelhard, M.; Wachtveitl, J. First steps of retinal photoisomerization in proteorhodopsin. *Biophys. J.* **2006**, *91* (1), 255–262.

(9) Rupenyan, A.; van Stokkum, I. H. M.; Arents, J. C.; van Grondelle, R.; Hellingwerf, K.; Groot, M. L. Characterization of the Primary Photochemistry of Proteorhodopsin with Femtosecond Spectroscopy. *Biophys. J.* **2008**, *94* (10), 4020–4030.

(10) Amsden, J. J.; Kralj, J. M.; Bergo, V. B.; Spudich, E. N.; Spudich, J. L.; Rothschild, K. J. Different Structural Changes Occur in Blue- and Green-Proteorhodopsins during the Primary Photoreaction. *Biochemistry* **2008**, *47* (44), 11490–11498.

(11) Kandori, H.; Katsuta, Y.; Ito, M.; Sasabe, H. Femtosecond fluorescence study of the rhodopsin chromophore in solution. *J. Am. Chem. Soc.* **1995**, *117* (9), 2669–2670.

(12) Logunov, S. L.; Song, L.; El-Sayed, M. A. Excited-State Dynamics of a Protonated Retinal Schiff Base in Solution. *J. Phys. Chem.* **1996**, *100* (47), 18586–18591.

(13) Freedman, K. A.; Becker, R. S. Comparative investigation of the photoisomerization of the protonated and unprotonated n-butylamine Schiff bases of 9-cis-, 11-cis-, 13-cis-, and all-trans-retinals. *J. Am. Chem. Soc.* **1986**, *108* (6), 1245–1251.

(14) Chosrowjan, H.; Mataga, N.; Shibata, Y.; Tachibanaki, S.; Kandori, H.; Shichida, Y.; Okada, T.; Kouyama, T. Rhodopsin Emission in Real Time: A New Aspect of the Primary Event in Vision. *J. Am. Chem. Soc.* **1998**, *120* (37), 9706–9707.

(15) Xu, D.; Martin, C.; Schulten, K. Molecular dynamics study of early picosecond events in the bacteriorhodopsin photocycle: dielectric response, vibrational cooling and the J, K intermediates. *Biophys. J.* **1996**, *70* (1), 453–460.

(16) Huber, R.; Kohler, T.; Lenz, M. O.; Bamberg, E.; Kalmbach, R.; Engelhard, M.; Wachtveitl, J. pH-dependent photoisomerization of retinal in proteorhodopsin. *Biochemistry* **2005**, *44* (6), 1800–1806.

(17) Ruhman, S.; Hou, B.; Friedman, N.; Ottolenghi, M.; Sheves, M. Following Evolution of Bacteriorhodopsin in Its Reactive Excited State via Stimulated Emission Pumping. *J. Am. Chem. Soc.* **2002**, *124* (30), 8854–8858.

(18) Haruki, I.; Chioko, N.; Naohiko, M.; Robert, W. F. Observation of the "isomerization states" of HCP by stimulated emission pumping spectroscopy: Comparison between theory and experiment. *J. Chem. Phys.* **1997**, *106* (7), 2980–2983.

(19) Yan, M.; Rothberg, L.; Callender, R. Femtosecond Dynamics of Rhodopsin Photochemistry Probed by a Double Pump Spectroscopic Approach. *J. Phys. Chem. B* **2001**, *105* (4), 856–859.

(20) Wohlleben, W.; Buckup, T.; Hashimoto, H.; Cogdell, R. J.; Herek, J. L.; Motzkus, M. Pump-Deplete-Probe Spectroscopy and the Puzzle of Carotenoid Dark States. *J. Phys. Chem. B* **2004**, *108* (10), 3320–3325.

(21) Kennis, J. T. M.; Larsen, D. S.; van Stokkum, I. H. M.; Vengris, M.; van Thor, J. J.; van Grondelle, R. Uncovering the hidden ground state of green fluorescent protein. *Proc. Natl. Acad. Sci. U.S.A.* **2004**, *101* (52), 17988–17993.

(22) Gai, F.; McDonald, J. C.; Anfinrud, P. A. Pump-Dump-Probe Spectroscopy of Bacteriorhodosin: Evidence for a Near-IR Excited State Absorbance. *J. Am. Chem. Soc.* **1997**, *119* (26), 6201–6202.

(23) Meyer, T. E.; Tollin, G.; Hazzard, J. H.; Cusanovich, M. A. Photoactive yellow protein from the purple phototrophic bacterium, Ectothiorhodospira halophilaQuantum yield of photobleaching and effects of temperature, alcohols, glycerol, and sucrose on kinetics of photobleaching and recovery. *Biophys. J.* **1989**, *56* (3), 559–564.

(24) Larsen, D. S.; van Stokkum, I. H. M.; Vengris, M.; van der Horst, M. A.; de Weerd, F. L.; Hellingwerf, K. J.; van Grondelle, R. Incoherent manipulation of the photoactive yellow protein photocycle with dispersed pump-dump-probe spectroscopy. *Biophys. J.* **2004**, *87* (3), 1858–1872.

(25) van Wilderen, L. J. G. W.; van der Horst, M. A.; van Stokkum, I. H. M.; Hellingwerf, K. J.; van Grondelle, R.; Groot, M. L. Ultrafast infrared spectroscopy reveals a key step for successful entry into the photocycle for photoactive yellow protein. *Proc. Natl. Acad. Sci. U.S.A.* **2006**, *103* (41), 15050–15055.

(26) Friedrich, T.; Geibel, S.; Kalmbach, R.; Chizhov, I.; Ataka, K.; Heberle, J.; Engelhard, M.; Bamberg, E. Proteorhodopsin is a light-driven proton pump with variable vectoriality. *J. Mol. Biol.* **2002**, *321* (5), 821–838.

(27) van Stokkum, I. H. M.; Larsen, D. S.; van Grondelle, R. Global and target analysis of time-resolved spectra. *Biochim. Biophys. Acta, Bioenerg.* **2004**, *1657* (2−3), 82–104.

(28) Lenz, M. O.; Woerner, A. C.; Glaubitz, C.; Wachtveitl, J. Photoisomerization in proteorhodopsin mutant D97N. *Photochem. Photobiol.* **2006**, *83*, 226−231.

(29) Gai, F.; Hasson, K. C.; McDonald, J. C.; Anfinrud, P. A. Chemical Dynamics in Proteins: The Photoisomerization of Retinal in Bacteriorhodopsin. *Science* **1998**, *279* (5358), 1886–1891.

(30) Bajaj, V. S.; Mak-Jurkauskas, M. L.; Belenky, M.; Herzfeld, J.; Griffin, R. G. Functional and shunt states of bacteriorhodopsin resolved by 250 GHz dynamic nuclear polarization-enhanced solid-state NMR. *Proc. Natl. Acad. Sci. U.S.A.* **2009**, *106* (23), 9244–9249.

(31) McCamant, D. W.; Kukura, P.; Mathies, R. A. Femtosecond Stimulated Raman Study of Excited-State Evolution in Bacteriorhodopsin. *J. Phys. Chem. B* **2005**, *109* (20), 10449–10457.

(32) Kakitani, H.; Kakitani, T.; Rodman, H.; Honig, B.; Callender, R. Correlation of Vibrational Frequencies with Absorption Maxima in Polyenes, Rhodopsin, Bacteriorhodopsin, and Retinal Analogs. *J. Phys. Chem.* **1983**, *87* (19), 3620–3628.

JP9065289